Journal of Alloys and Compounds 504S (2010) S27–S30

Contents lists available at ScienceDirect

Journal of Alloys and Compounds

journal homepage: www.elsevier.com/locate/jallcom

Improvement of glass-forming ability and phase separation in Cu–Ti-rich Cu–Ti–Zr–Ni–Si bulk metallic glasses

E.S. Park[a,*], H.J. Chang[b], D.H. Kim[c]

[a] Research Institute of Advanced Materials, Department of Materials Science and Engineering, Seoul National University, Seoul 151-744, Republic of Korea
[b] Materials Science and Technology Division, Oak Ridge National Laboratory, Oak Ridge, TN37831, United States
[c] Center for Non-crystalline Materials, Department of Metallurgical Engineering, Yonsei University, Seoul 120-749, Republic of Korea

ARTICLE INFO

Article history:
Received 4 July 2009
Received in revised form 19 April 2010
Accepted 24 April 2010
Available online 10 July 2010

Keywords:
Metallic glass
Liquid quenching
Phase separation

ABSTRACT

Present study reports improvement of glass-forming ability (GFA) and phase separation in Cu–Ti-rich Cu–Ti–Zr–Ni–Si bulk metallic glasses (BMGs) by tailoring the constituent elements. The MA of metalloid element, Sn having relatively large negative enthalpy of mixing can lead to improve GFA (up to 8 mm in diameter) as well as thermal stability (up to $\Delta T_x = 48$ K) by optimizing the substitution element. And the addition of elements having relatively large positive enthalpy of mixing (partial substitution of Zr or Ti with Y) can lead to the liquid state phase separation in Cu–Ti–Sn–Zr–Ni–Si BMG, although the addition lead to drastic deterioration of the GFA.

1. Introduction

The glass-forming ability (GFA) and properties of bulk metallic glasses (BMGs) are quite responsible to the variation of internal factors such as the number of components, the atomic size, the purity, the composition and the cohesion between the metals. Thus, the tailoring constituent elements have already played the effective and crucial roles in glass formation, improvement of thermal stability and properties of BMGs even at the beginning of the birth of BMGs [1]. However, we are still far away from pinpointing compositions with both optimized GFA and desirable properties. In particular, it is still an unraveled mystery that a minor addition (MA) of alloying elements or a small change in composition can drastically change the properties as well as the GFA.

Cu–Ti-rich Cu–Ti–Zr–Ni(–Si) alloys as a class of low-cost BMGs exhibit high GFA over a wide composition ranges (up to 4 mm in diameter), interesting room temperature fracture strength (σ_f ~2 GPa), high Young's modulus of about 120 GPa as well as rather large compressive plastic strain up to ~2% [2,3]. There have been some studies to explore the improvement of GFA, thermal stability and properties in Cu–Ti–Zr–Ni(–Si) BMG by substituting minor elements, i.e., partial substitution of Ni with Sn or In to increase the attainable maximum thickness [4,5], partial substitution of Zr with Nb to improve the plasticity [6,7], and even small addition of Mo or W to enhance the corrosion resistance [8]. However, the systematical approach for optimizing GFA and tailoring properties in Cu–Ti-rich BMGs is limited, except a few tentative discussions [2–10]. Therefore, in the present study, we further revealed the role of tailoring constituent elements in Cu–Ti-rich Cu–Ti–Zr–Ni–Si BMGs by considering the combination of mixing enthalpies of the atomic pairs. As a result, first we show that MA of metalloid element, Sn having relatively large negative enthalpy of mixing with constituent elements can lead to the improvement of GFA (up to 8 mm in diameter) as well as thermal stability (up to $\Delta T_x = 48$ K) by optimizing substitution element. Secondly, the addition of elements having relatively large positive enthalpy of mixing (partial substitution of Zr or Ti with Y; Y–Zr: +35 kJ/mol, Y–Ti: +58 kJ/mol [11]) can lead to the liquid state phase separation in Cu–Ti–Sn–Zr–Ni–Si BMGs, although the addition lead to drastic deterioration of the GFA.

2. Experimental

Cu–Ti–Zr–Ni–Si–M (M = Sn and Y) alloy ingots were produced by arc melting under a Ti-gettered argon atmosphere in a water cooled copper crucible. Rapidly solidified and injection-cast specimens were prepared by re-melting the alloys in quartz tubes, and ejecting with an over-pressure of 50 kPa through a nozzle onto a Cu wheel rotating with a surface velocity of 40 m/s and into the Cu mold having cylindrical cavities of 1–9 mm in diameter.

The structure of the samples was examined preliminarily by X-ray diffraction (XRD, Rigaku CN2301, Tokyo, Japan) using monochromatic Cu Kα radiation for a 2θ range of 20–80°. Thermal analysis of the samples was carried out to determine the glass transition temperature, T_g, and the crystallization onset temperature, T_x, by differential scanning calorimetry (DSC, PerkinElmer DSC7, Boston, MA) using a constant heating rate of 0.667 K/s. The microstructures of the samples were examined using the transmission electron microscopy (TEM, JEM 2100FX, 200 kV, Tokyo, Japan) linked with a high angle annular dark field (HAADF) detector. The thin foil

* Corresponding author. Tel.: +82 2 880 7221; fax: +82 2 883 8197.
E-mail address: espark@snu.ac.kr (E.S. Park).

0925-8388/$ – see front matter © 2010 Elsevier B.V. All rights reserved.
doi:10.1016/j.jallcom.2010.04.129

specimens for TEM were prepared by Ar ion milling using Gatan, Model 600 (Vienna, OH) at 2.6 keV and ~5 mA with liquid nitrogen cooling. Extreme care was taken with the TEM analysis since Cu-based metallic glass thin foils oxidize readily upon exposure to air.

3. Results and discussion

3.1. Minor addition of metalloid element, Sn

Metalloid elements have a strong affinity with conventional BMG-forming alloying elements such as Cu, Zr, Ti, Fe, Mg and rare earth elements, i.e., they have relatively large negative enthalpy of mixing with these elements. The metalloid elements can react with the main metallic constituents and form thermodynamically favored crystalline compounds with a high melting temperature [1]. Therefore, it is expected that the metalloid elements would result in crystallization and degrade the GFA of the BMG-forming alloys. However, the proper additions can cause more densely packed structure and then stabilize the alloy against the crystallization. Fig. 1 shows DSC traces obtained from rapidly solidified (a) $Cu_{47}Ti_{34}Zr_{11}Ni_8$, (b) $Cu_{47}Ti_{33}Zr_{11}Ni_8Si_1$, (c) $Cu_{47}Ti_{33}Zr_{11}(Ni_6Sn_2)Si_1$, (d) $(Cu_{45}Sn_2)Ti_{33}Zr_{11}Ni_8Si_1$, (e) $Cu_{47}Ti_{33}(Zr_9Sn_2)Ni_2Si_1$ and (f) $Cu_{47}(Ti_{31}Sn_2)Zr_{11}Ni_8Si_1$ ribbons. As reported previously, MAs of Si and Sn make the alloys more thermally stable [2,4]. The T_g and T_x increased from 702 K and 737 K, respectively at alloy (a) to 720 K and 757 K, respectively at alloy (b) and up to 720 K and 765 K, respectively at alloy (c). With MA of metalloid elements, Si and Sn, the supercooled liquid region, $\Delta T_x = T_x - T_g$, also increased from 37 K at alloy (a) up to 45 K at alloy (c). Interestingly, as shown in Fig. 1(c)–(f), thermal stability and crystallization behavior were changed depending on the substitution elements with Sn in $Cu_{47}Ti_{33}Zr_{11}Ni_8Si_1$ BMG. The small substitution of Ti with Sn (2 at.%) exhibits most stable thermal stability with 722 K of T_g, 770 K of T_x and 48 K of ΔT_x,

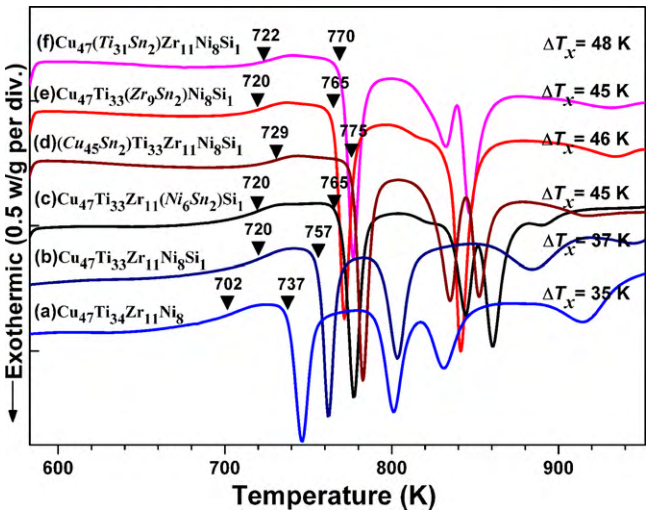

Fig. 1. DSC traces obtained from rapidly solidified Cu–Ti-rich Cu–Ti–Zr–Ni(–Si–Sn) ribbons.

respectively. Fig. 2 shows the XRD patterns obtained from injection cast (a) $Cu_{47}Ti_{33}Zr_{11}(Ni_6Sn_2)Si_1$, (b) $(Cu_{45}Sn_2)Ti_{33}Zr_{11}Ni_8Si_1$, (c) $Cu_{47}Ti_{33}(Zr_9Sn_2)Ni_2Si_1$ and (d) $Cu_{47}(Ti_{31}Sn_2)Zr_{11}Ni_8Si_1$ alloy samples with different diameters. As reported previously, XRD pattern for $d = 7$ mm specimen of alloy (a) showed several sharp diffraction peaks superimposed on a weak broad halo pattern, clearly indicating the maximum diameter for glass formation (D_{max}) is below 7 mm in diameter ($D_{max} = 6$ mm [4]). On the other hand, XRD pattern for $d = 7$ mm specimen of alloy (b) showed fewer sharp diffraction peaks superimposed on a strong broad halo pattern, clearly indicating the formation of a mixture of amorphous and crystalline phase ($D_{max} < 7$ mm). Interestingly, in alloy (c) the

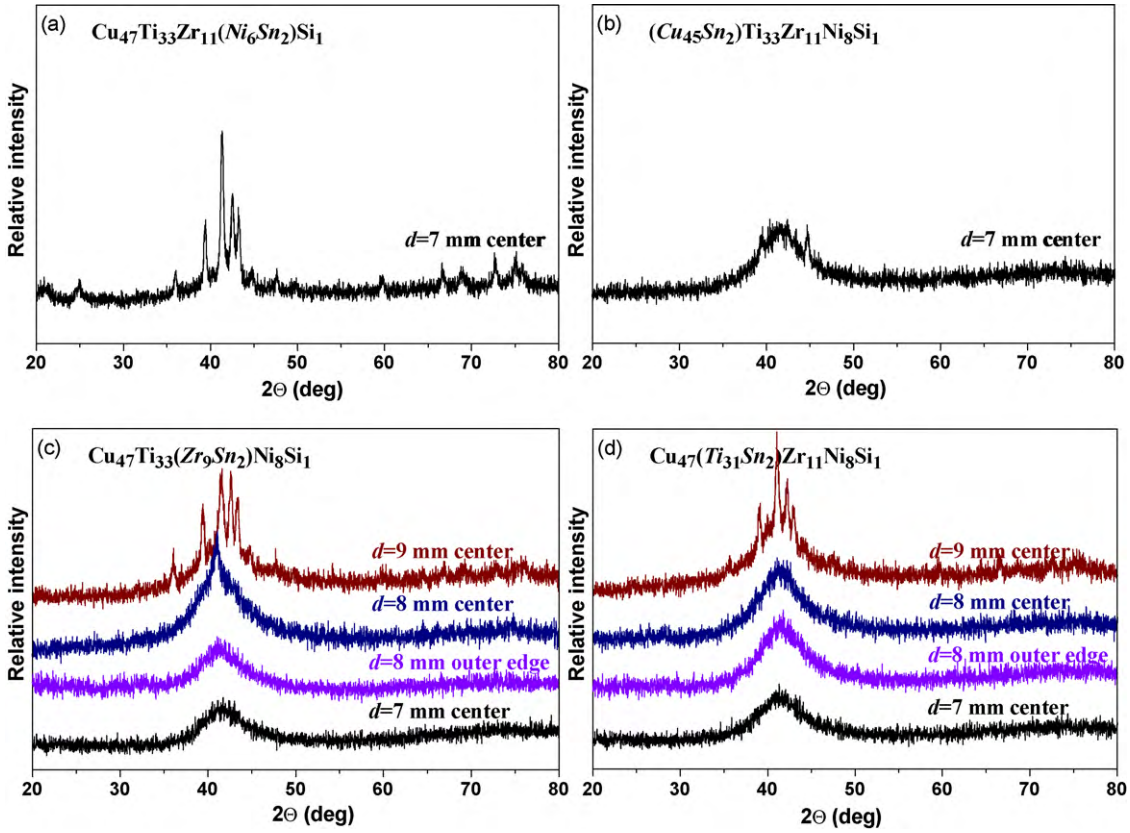

Fig. 2. XRD patterns obtained from injection-cast bulk specimens with different diameters in Cu–Ti–Zr–Ni–Si–Sn alloys.

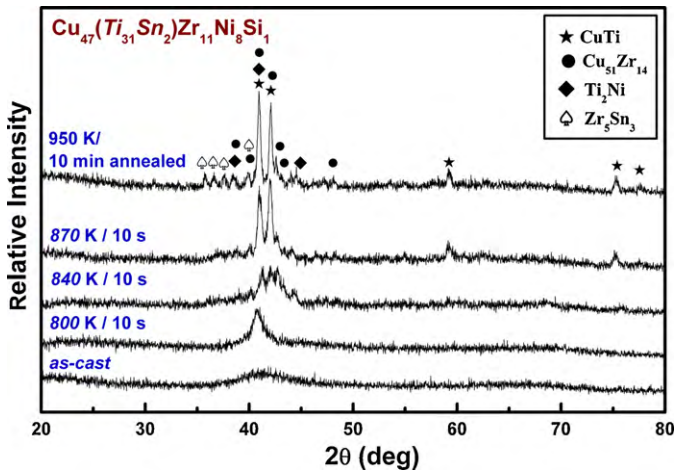

Fig. 3. XRD traces obtained from the as-cast and annealed $Cu_{47}(Ti_{31}Sn_2)Zr_{11}Ni_8Si_1$ rod sample with 8 mm in diameter.

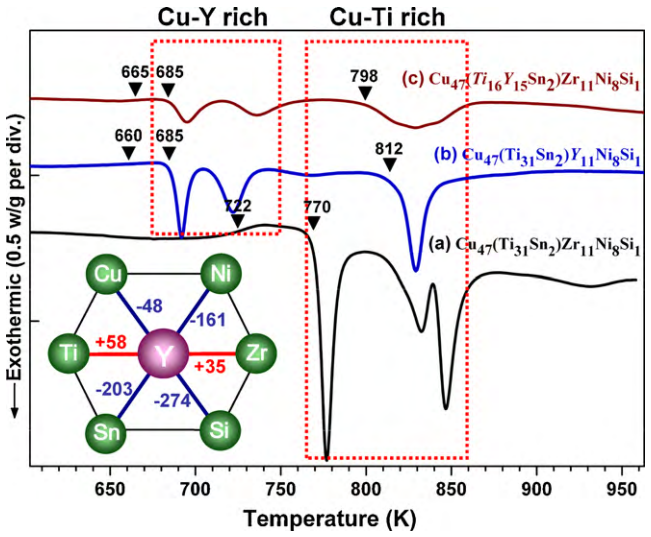

Fig. 4. DSC traces obtained from rapidly solidified (a) $Cu_{47}(Ti_{31}Sn_2)Zr_{11}Ni_8Si_1$, (b) $Cu_{47}(Ti_{31}Sn_2)Y_{11}Ni_8Si_1$ and (c) $Cu_{47}(Ti_{16}Y_{15}Sn_2)Zr_{11}Ni_8Si_1$ ribbons. The inset shows relationship of heat of fusion among Y and constituent elements in Cu–Ti–Sn–Zr–Ni–Si–Y alloy system.

partial substitution of Zr with Sn promoted GFA below 8 mm in diameter (D_{max} < 8 mm) and in alloy (d) the partial substitution Ti with Sn improved GFA up to 8 mm in diameter (D_{max} = 8 mm). This result indicates that the optimization of substitution elements can lead to the improved GFA of the BMG forming-alloy system.

In order to identify the crystallization products for each exothermic reaction, annealing treatments were performed. Fig. 3 shows typical XRD traces obtained from the as-cast and annealed $Cu_{47}(Ti_{31}Sn_2)Zr_{11}Ni_8Si_1$ rod sample with 8 mm in diameter. The XRD trace obtained from the $Cu_{47}(Ti_{31}Sn_2)Zr_{11}Ni_8Si_1$ rod annealed for 10 s at 800 K, i.e., after the first exothermic reaction, showed relatively sharpened diffraction peak. With increasing annealing temperature, several sharp diffraction peaks, which are related to formation of crystalline phases can be detected. Finally, the XRD trace obtained from the $Cu_{47}(Ti_{31}Sn_2)Zr_{11}Ni_8Si_1$ rod annealed for 10 min at 950 K, i.e., after all exothermic reactions, showed several sharp diffraction peaks from a mixture of CuTi (tetragonal), $Cu_{51}Zr_{14}$ (hexagonal), Ti_2Ni (cubic), and Zr_5Sn_3 (hexagonal). In particular, it can be understood that minor addition of Sn in Cu–Ti–Zr–Ni–Si cause to formation of supplementary Zr_5Sn_3 phase (hexagonal structure, a = 8.46 Å, c = 5.79 Å), which is same structure with $Cu_{51}Zr_{14}$, competing crystalline phase of Cu–Ti–Zr–Ni–Si BMG. Thus, it can be analogized that the formation of Zr_5Sn_3 phase might disturb for the formation of $Cu_{51}Zr_{14}$, which can be one of the crucial roles for the improvement of GFA. Furthermore, the simultaneous precipitation of the multiple crystallized phases also results in the redistribution of the constituent elements on long-range scale, thus improving GFA [12].

The present results show that the optimized substitution of Sn in Cu–Ti-rich Cu-based BMGs can increase their critical diameter for glass formation. A large size difference between Sn and the other constituent elements is favorable to increase the atomic packing density of the liquid structure and in incompatible with the preferred atomic size ratio of the Laves phases, thus suppressing the formation of this phase. Furthermore, the larger negative enthalpies of mixing between Sn and other constituent elements (Sn–Cu, Sn–Ti, Sn–Zr and Sn–Ni are −13, −139, −201 and −21 kJ/mol, respectively) [11] can contribute to the stabilization of the liquid phase by changing the local atomic structure. It should be mentioned that large replacement of Sn (>2 at.%) decreased the GFA, which might be closely related to formation of thermodynamically favored crystalline compounds. In particular, the GFA of the Cu-based alloys are very sensitive to the substitution elements with Sn, although all Cu–Ti–Zr–Ni–Si–Sn alloys show the similar stable thermal stability as well as relaxation kinetics of the supercooled liquid. The substitution Ti and Zr rather than Cu and Ni with Sn exhibit better GFA. This results indicate that the role of oxygen in our Cu based BMGs is critical as in other Ti and Zr based BMGs since most of the oxygen in our alloy is introduced by Ti and Zr (350–400 ppm oxygen (weight concentration)) which can dissolve O, while Cu does not dissolve O according to the binary equilibrium phase diagram [9]. In this alloy system, Zr- and Ti-oxides are chemically more stable and structurally denser than Ni- and Cu-oxide, which can be considered to act as a heterogeneous nucleation sites [8]. In the Ni–Pd–P alloy system, the improvement of the GFA by adding Si is attributed to the destabilization of P_2O_5 clusters [13], and in the similar way, in our Cu–Ti-rich BMGs, Sn might act and help to destabilize predominant TiO_2 clusters present in the melt.

3.2. Tailored substitution of Y with Zr or Ti

Phase separation in the liquid state has been experimentally observed when large repulsive interactions are present between two major constituent elements. The preparation of a phase separating metallic glass requires modifying the alloy with high GFA by addition of an element with a strong repulsive tendency to one of the constituent elements [14–25]. To obtain further insight, an alloying element Y having relatively large positive enthalpy of mixing with Zr or Ti (Y–Zr: +35 kJ/mol, Y–Ti: +58 kJ/mol) was added in $Cu_{47}(Ti_{31}Sn_2)Zr_{11}Ni_8Si_1$ (D_{max} = 8 mm) alloys. The inset shows relationship of heat of fusion among Y and constituent elements in Cu–Ti–Sn–Zr–Ni–Si–Y BMG system. Fig. 4 shows DSC traces obtained from rapidly solidified (a) $Cu_{47}(Ti_{31}Sn_2)Zr_{11}Ni_8Si_1$, (b) $Cu_{47}(Ti_{31}Sn_2)Y_{11}Ni_8Si_1$ and (c) $Cu_{47}(Ti_{16}Y_{15}Sn_2)Zr_{11}Ni_8Si_1$ ribbons during heating with a heating rate of 0.667 K/s. With adding Y elements, T_g and T_x dramatically decreased such as from T_x = 772 K at alloy (a) down to T_x = 685 K at alloys (b) and (c). Thus, the DSC traces can be clearly classified into two groups based on the temperature range of the exothermic reaction, i.e., low temperature ranges with T_x in the range 685 K (referred to as peak I) and high-temperature exothermic reactions with T_x in the range 798 K to 812 K (referred to as peak II). XRD results on the samples, heated up to 760 K and 900 K (not shown), indicated that the exothermic reactions related to peak I and peak II corresponded to the crystallization of Cu–Y-rich and Cu–Ti-rich amorphous phase respectively. Considering the higher crystallization temperature for the Cu–Ti-rich amorphous

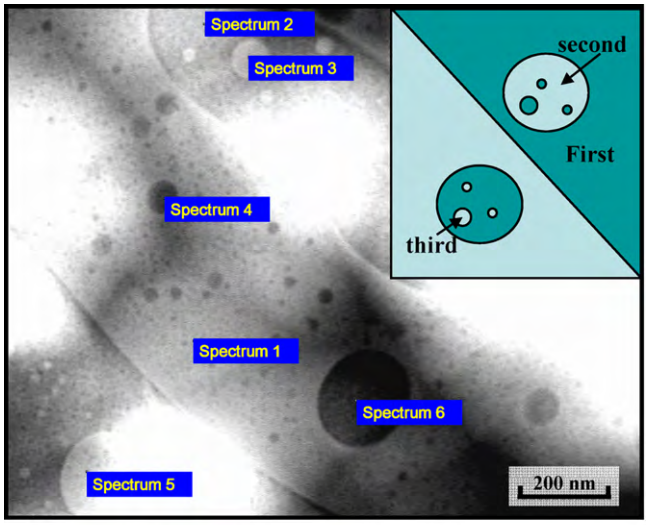

Spectrum	Cu	Ti	Sn	Y	Ni	Si	Phase
1	33.75	42.83	1.02	1.92	12.39	8.10	1st Cu-Ti-rich
2	61.47	5.28	2.77	19.46	1.36	9.66	1st Cu-Y-rich
3	31.53	45.08	0.59	0.77	13.51	8.52	2nd Cu-Ti-rich
4	60.85	5.34	3.70	19.07	2.64	8.40	2nd Cu-Y-rich
5	30.93	43.10	0.42	1.38	13.78	10.39	2nd Cu-Ti-rich
6	63.53	3.96	3.33	20.61	1.06	7.51	2nd Cu-Y-rich

Fig. 5. Z-contrast image of the rapidly solidified $Cu_{47}(Ti_{31}Sn_2)Y_{11}Ni_8Si_1$ ribbon. The inset shows schematic diagram of hierarchical structure obtained from continuous phase separation. The table summarizes the measured compositions for both darker (Cu–Y-rich) and brighter (Cu–Ti-rich) hierarchical droplets.

phase, first Cu–Ti-rich liquid vitrifies into the amorphous phase, and then the remaining Cu–Y-rich liquid vitrifies into the amorphous phase at a low temperature. The results indicate that an increase of Y content in the Cu–Ti–Zr–Ni–Si(–Sn) alloys moves the alloy composition toward the miscibility gap region, thereby forming two different amorphous phases by separation in the liquid state during cooling. The two T_xs are apart by about 100 K, which is large enough to exhibit two independent crystallization sequences for the two phases. On the one hand, addition of Y causes dramatic deterioration of GFA down to below 1 mm in diameter (not shown). In particular, substitution Ti with Y causes easier deterioration of GFA than substitution Zr with Y in $Cu_{47}(Ti_{31}Sn_2)Zr_{11}Ni_8Si_1$ BMG. This result indicates that the development of a phase separating metallic glass faces an apparent paradox with the GFA.

To confirm the occurrence of phase separation with compositional difference, intensive structural analysis for the rapidly solidified $Cu_{47}(Ti_{31}Sn_2)Y_{11}Ni_8Si_1$ ribbon was performed by Z-contrast observation as shown in Fig. 5. The Z-contrast image clearly shows the presence of two different amorphous phases with darker and brighter contrasts. The smooth interface between both regions (darker and brighter) indicates that separation occurred in the liquid state. Both regions are not single phase and exhibit surface fractal structure with some features of self-similarity during continuous cooling. The inset of Fig. 5 clearly shows the schematic diagram of hierarchical structure obtained from continuous phase separation. The large droplets of secondary separation have a size of up to 200 nm, while the finer droplets of third separation have a size of down to 10 nm. The measured compositions of hierarchical structure are summarized in Table of Fig. 5. The average compositions of darker and brighter droplets are Cu–Y-rich $Cu_{62}Ti_5Sn_3Y_{20}Ni_2Si_8$ and Cu–Ti-rich $Cu_{32}Ti_{44}Sn_1Y_1Ni_{13}Si_9$, respectively, confirming that peaks I and II of the DSC trace correspond to crystallization of Cu–Y-rich and Cu–Ti-rich amorphous phases. Although it can be generally expected that the compositional range will be narrower in smaller spheres, which form at the latest stage in the cooling sequence, in the present study, the average compositions of both darker and brighter hierarchical droplets are almost similar within the experimental error. This result might be rationalized that the slope of miscibility gap should be quite steep in the decomposition temperature ranges, since the range of local compositions changes strongly depending on the slope of the miscibility gap curve. Although this finding is still only inferiorly understood, this approach is considered to be effective in the tailored design of a novel class *in situ* composite.

4. Conclusion

The present study shows that tailoring constituent elements by considering the combination of mixing enthalpies of the atomic pairs can cause improved GFA and phase separation in Cu–Ti–Zr–Ni–Si BMG. First, the MA of metalloid element, Sn having relatively large negative enthalpy of mixing with constituent elements can lead to the improvement of GFA (up to $D_{max} = 8$ mm) as well as thermal stability (up to $\Delta T_x = 48$ K) by selecting the substitution element as Ti. Secondly, the MA of elements having relatively large positive enthalpy of mixing (partial substitution of Zr or Ti with Y) can lead to the liquid state phase separation in Cu–Ti–Sn–Zr–Ni–Si–Y BMGs, although the addition leads to drastic deterioration of GFA. This concept would be considered to be effective even in the design of other BMG systems with desirable properties.

Acknowledgements

This work was supported by the Global Research Laboratory Program of the Korean Ministry of Science. One of the authors (E.S. Park) was supported by the Center for Iron and Steel Research at Research Institute of Advanced Materials (RIAM) and Engineering Research Institute at Seoul National University.

References

[1] W.H. Wang, Prog. Mater. Sci. 52 (2007) 540–596.
[2] H. Choi-Yim, R. Busch, W.L. Johnson, J. Appl. Phys. 83 (1998) 7993.
[3] M. Calin, J. Eckert, L. Schultz, Scripta Mater. 48 (2003) 653–658.
[4] E.S. Park, H.K. Lim, W.T. Kim, D.H. Kim, J. Non-Cryst. Solids 298 (2002) 15–22.
[5] E.S. Park, W.T. Kim, D.H. Kim, Mater. Trans. 45 (2004) 2693–2696.
[6] E.S. Park, D.H. Kim, T. Ohkubo, K. Hono, J. Non-Cryst. Solids 351 (2005) 1232–1238.
[7] E.S. Park, H.J. Chang, J.S. Kyeong, D.H. Kim, J. Mater. Res. 23 (2008) 1995–2002.
[8] B. Liu, L. Liu, Mater. Sci. Eng. A 415 (2006) 286–290.
[9] S. Venkataraman, M. Stoica, S. Scudino, T. Gemming, C. Mickel, U. Kunz, K.B. Kim, L. Schultz, J. Eckert, Scripta Mater. 54 (2006) 835–840.
[10] E.S. Park, D.H. Kim, Met. Mater. Int. 11 (2005) 19–27.
[11] A.R. Miedema, Philips Tech. Rev. 36 (1976) 217–231.
[12] A. Inoue, T. Zhang, T. Masumoto, J. Non-Cryst. Solids 156–158 (1993) 473–480.
[13] C.A. Volkert, Ph.D. Thesis, Harvard University (1988).
[14] A.A. Kündig, M. Ohnuma, D.H. Ping, T. Ohkubo, K. Hono, Acta Mater. 52 (2004) 2441–2448.
[15] B.J. Park, H.J. Chang, W.T. Kim, D.H. Kim, Appl. Phys. Lett. 85 (2004) 6353.
[16] N. Mattern, U. Kühn, A. Gebert, T. Gemming, M. Zinkevich, H. Wendrock, L. Schultz, Scripta Mater. 53 (2005) 271–274.
[17] E.S. Park, D.H. Kim, Acta Mater. 54 (2006) 2597–2604.
[18] B.J. Park, H.J. Chang, D.H. Kim, W.T. Kim, K. Chattopadhyay, T.A. Abinandanan, S. Bhattacharyya, Phys. Rev. Lett. 96 (2006) 245503.
[19] E.S. Park, E.Y. Jeong, J.-K. Lee, J.C. Bea, A.R. Kwon, A. Gebert, L. Schultz, H.J. Chang, D.H. Kim, Scripta Mater. 56 (2007) 197–200.
[20] E.S. Park, J.S. Kyeong, D.H. Kim, Scripta Mater. 57 (2007) 49–52.
[21] E.S. Park, H.J. Chang, J.Y. Lee, D.H. Kim, J. Mater. Res. 22 (2007) 3440–3447.
[22] E.S. Park, H.J. Chang, D.H. Kim, Acta Mater. 56 (2008) 3120–3131.
[23] J.H. Na, Y.C. Kim, W.T. Kim, D.H. Kim, Met. Mater. Int. 14 (2008) 553–557.
[24] H.J. Chang, W. Yook, E.S. Park, J.S. Kyeong, D.H. Kim, Acta Mater. 58 (2010) 2483–2491.
[25] H.J. Chang, E.S. Park, W. Yook, D.H. Kim, in press.